Thermodynamic Studies to Support Actinide/Lanthanide Separations

Fuel Cycle Research & Development

Prepared for
U.S. Department of Energy
Materials Recovery and Waste Form Development

Linfeng Rao
Lawrence Berkeley National Laboratory

September 2016

FCRD-MRWFD-2016-000346
LBNL-1006035

Revision 2
12/20/2012

APPENDIX E

FCT DOCUMENT COVER SHEET [1]

Name/Title of Deliverable/Milestone/Revision No.	Thermodynamic Studies to Support Actinide/Lanthanide Separations
Work Package Title and Number	Thermodynamics and Kinetics – LBNL FT-16LB03010403
Work Package WBS Number	1.02.03.01.04
Responsible Work Package Manager	Linfeng Rao (Signature on file)
	(Name/Signature)

Date Submitted 9/4/2016

Quality Rigor Level for Deliverable/Milestone[2]	☐ QRL-3	☐ QRL-2	☐ QRL-1 ☐ Nuclear Data	x Lab/Participant QA Program (no additional FCT QA requirements)

This deliverable was prepared in accordance with Lawrence Berkeley National Laboratory
(Participant/National Laboratory Name)

QA program which meets the requirements of
☒ DOE Order 414.1 ☐ NQA-1-2000 ☐ Other

This Deliverable was subjected to:

☒ Technical Review ☐ Peer Review

Technical Review (TR)

Review Documentation Provided

☐ Signed TR Report or,
☐ Signed TR Concurrence Sheet or,
☒ Signature of TR Reviewer(s) below

Peer Review (PR)

Review Documentation Provided

☐ Signed PR Report or,
☐ Signed PR Concurrence Sheet or,
☐ Signature of PR Reviewer(s) below

Name and Signature of Reviewers

Zhicheng Zhang (Signature on file)

NOTE 1: *Appendix E should be filled out and submitted with the deliverable. Or, if the PICS:NE system permits, completely enter all applicable information in the PICS:NE Deliverable Form. The requirement is to ensure that all applicable information is entered either in the PICS:NE system or by using the FCT Document Cover Sheet.*

NOTE 2: *In some cases there may be a milestone where an item is being fabricated, maintenance is being performed on a facility, or a document is being issued through a formal document control process where it specifically calls out a formal review of the document. In these cases, documentation (e.g., inspection report, maintenance request, work planning package documentation or the documented review of the issued document through the document control process) of the completion of the activity along with the Document Cover Sheet is sufficient to demonstrate achieving the milestone. If QRL 1, 2, or 3 is not assigned, then the Lab/Participant QA Program (no additional FCT QA requirements) box must be checked, and the work is understood to be performed, and any deliverable developed, in conformance with the respective National Laboratory/Participant, DOE- or NNSA-approved QA Program.*

This page is intentionally blank.

SUMMARY

Thermodynamic data on the complexation of Np(V) with HEDTA in a wide pH region were re-modeled by including a dimeric complex species, $(NpO_2)_2(OH)_2L_2^{6-}$ where L^{3-} stands for the fully deprotonated HEDTA ligand and better fits were achieved for the spectrophotometric data. The presence of the dimeric complex species in high pH region was verified for the first time by the EXAFS experiments at Stanford Synchrotron Radiation Laboratory (SSRL).

CONTENTS

FIGURES

TABLES

ACRONYMS

DTPA	diethyltriaminepentaacetic acid
EXAFS	extended x-ray absorption fine structure
HDEHP	bis-2-ethyl(hexyl) phosphoric acid
HEDTA	N-(2-hydroxyethyl) ethylenediamine-N,N',N'-triacetic acid
HEH[EHP]	2-ethyl (hexyl) phosphonic acid mono-2-ethylhexyl ester
IDA	iminodiacetic acid
NEA	Nuclear Energy Agency
NE FCRD	Nuclear Energy Fuel Cycle Research and Development
NTA	nitrilotriacetic acid
TALSPEAK	Trivalent Actinide Lanthanide Separations by Phosphorus-reagent Extraction from Aqueous Komplexes

1. INTRODUCTION

In the modified TALSPEAK process, 2-ethyl (hexyl) phosphonic acid mono-2-ethylhexyl ester (HEH[EHP]) is proposed to be used as the extractant in the organic phase to replace bis-2-ethyl(hexyl) phosphoric acid (HDEHP), and a weaker aqueous complexant (N-(2-hydroxyethyl)ethylenediamine-N,N',N'-triacetic acid, HEDTA) is to be used to replace diethyltriaminepentaacetic acid (DTPA) in the aqueous phase. Preliminary studies have demonstrated that the combination of HEDTA with HEH[EHP] results in an almost flat pH dependence between 2.5 and 4.5, in contrast with conventional TALSPEAK. In addition, the HEDTA/HEH[EHP] combination has shown more rapid kinetics in phase transfer for the heavier lanthanides without using high concentrations of a lactate buffer as in the conventional TALSPEAK.

This milestone report summarizes the thermodynamic data on the complexation of Np(V) with HEDTA in a wide pH region, and the modelling of the data by including a dimeric complex species, $(NpO_2)_2(OH)_2L_2^{6-}$ where L^{3-} stands for the fully deprotonated HEDTA ligand. The model provides better fits for the spectrophotometric titration data. The presence of the dimeric complex species in high pH region was verified for the first time by the EXAFS experiments at Stanford Synchrotron Radiation Laboratory (SSRL).

2. RESULTS

2.1 Complexation of Np(V) with HEDTA

2.1.1 Complexation model and stability constants of Np(V)/HEDTA complexes constants

Figure 1 shows a representative spectrophotometric titration. Figure 1a shows a titration covering a wide pC_H (= -log [H^+]) range (3.0 to 11) while Figure 1b shows a titration where the highest pC_H is 5.5. In Figure 1a, the absorption band of free NpO_2^+ at 980.2 nm was red-shifted as HEDTA was added. Approximately three isosbestic points could be identified at 984, 990, and 994 nm, suggesting four absorbing species (free NpO_2^+ and three Np(V)/HEDTA complexes) were present in the titration solutions. A number of models were tested to fit the spectra data in the whole range of pC_H, including the model containing NpO_2L^{2-}, NpO_2HL^-, and $NpO_2(OH)L^{3-}$, but none were satisfactory. In some cases, a fit could converge but result in unreasonably large, negative absorptivities for the $NpO_2(OH)L^{3-}$ complex.

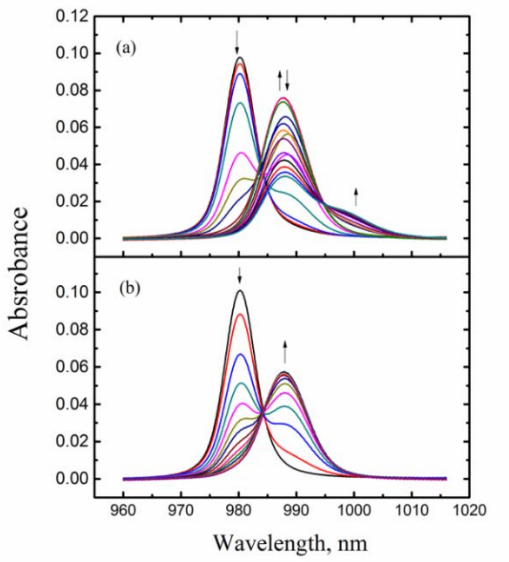

Figure 1. Spectrophotometric titrations of Np(V) with HEDTA at I = 1.0 mol·L^{-1} $NaClO_4$, t = 25 °C.

To better define the Np(V)/HEDTA complexes and obtain the stability constants, the titration data shown in Figure 1b that cover a narrower range of pC_H are processed first. Factor analysis of the spectra indicates the presence of three absorbing species and an excellent fit was achieved with the model including the formation of two Np(V)/HEDTA complexes: NpO_2L^{2-} and NpO_2HL^-, represented by reactions (1) and (2). The fit yielded the stability constants of log β_{101} (NpO_2L^{2-}) = 6.91 ± 0.06, and log $\beta_{1(11)}$ ($NpO_2(HL)^-$) = 4.28 ± 0.03.

$$NpO_2^+ + L^{3-} = NpO_2L^{2-} \quad (1)$$

$$NpO_2^+ + HL^{2-} = NpO_2HL^- \quad (2)$$

With the obtained stability constants of NpO_2L^{2-} and NpO_2HL^- as known values, the spectra from multiple titrations covering the whole range of pC_H (up to 11) were again fitted with models including an additional species that could become significant in basic solutions. In the fitting, the hydrolysis constants of the binary species, $NpO_2OH(aq)$ and $NpO_2(OH)_2^-$, were taken from the Nuclear energy agency (NEA) database and held constant. The model including the $NpO_2(OH)L^{3-}$ complex that was reported in the previous study did not converge. In contrast, the model including a dimeric species with the stoichiometry of $(NpO_2)_2(OH)_2L_2^{6-}$, resulted in a good fit with reasonable molar absorptivity. The formation of $(NpO_2)_2(OH)_2L_2^{6-}$ is represented by reaction (3), with an equilibrium constant of log $\beta_{2\text{-}22}$ ($(NpO_2)_2(OH)_2L_2^{6-}$) = -(4.93 ± 0.03).

$$2NpO_2^+ + 2L^{3-} + 2H_2O = (NpO_2)_2(OH)_2L_2^{6-} + 2H^+ \quad (3)$$

The equilibrium constants of reactions (1), (2), and (3) are summarized in Table 1. The equilibrium constants for reactions (1) and (2) from this work are in reasonable agreement with the values from previous studies, taking into consideration the difference in ionic strength. However, discrepancy exists in the model describing the data in the high pC_H region: the data in the present study are best represented by the formation of $(NpO_2)_2(OH)_2L_2^{6-}$ (reaction (3)), while the data from the previous study suggest the formation of $NpO_2(OH)L^{3-}$. The EXAFS results, which are obtained in the present work and will be discussed later, have demonstrated a dimeric Np(V) configuration in this ternary Np(V)-OH-HEDTA complex. Also, a ternary dimeric U(VI)-OH-IDA complex (IDA: iminodiacetic acid) has been suggested in the literature[26]. We thus believe that at the high pC_H area, Np(V) formed the ternary dimeric Np(V)-OH-HEDTA complex ($(NpO_2)_2(OH)_2L_2^{6-}$) with a similar configuration to that of the ternary dimeric U(VI)-OH-IDA complex, in which, each NpO_2^+ could be coordinated with one HEDTA ligand and the two NpO_2^+ centers are bridged by two hydroxides.

Table 1 Thermodynamic parameters of the Np(V) complexation with HEDTA at 25 °C in $NaClO_4$. Legends: sp – spectrophotometry, cal – calorimetry, pot – potentiometry, sx - solvent extraction, p.w.- present work.

Ligand	Reaction	I	Method	logβ	ΔH kJ·mol^{-1}	ΔS J·mol^{-1}·K^{-1}	ref
HEDTA	$NpO_2^+ + L^{3-} = NpO_2L^{2-}$	1.0 M	sp/cal	6.91 ± 0.06	-(8.0 ± 2.0)	105 ± 7	p.w.
	$NpO_2^+ + HL^{2-} = NpO_2HL^-$	1.0 M	sp/cal	4.28 ± 0.03	-(2.2 ± 2.0)	75 ± 7	p.w.
	$2NpO_2^+ + 2L^{3-} + 2H_2O = (NpO_2)_2(OH)_2L_2^{6-} + 2H^+$	1.0 M	sp	-(4.93 ± 0.03)			p.w.

2.1.2 Enthalpy of complexation

Three calorimetric titrations were conducted with both Np(V) and HEDTA in the initial cup solution titrated with $HClO_4$ or NaOH. The acid titrations covered the low pC_H range (8.5 – 3.5) so that the enthalpies of complexation for NpO_2L^{2-} and NpO_2HL^- were determined. The base titration extended the pC_H range up to 10.5 with the objective of obtaining the enthalpy of complexation for $(NpO_2)_2(OH)_2L_2^{6-}$.

Figure 2 shows the data of an acid titration. The reaction heats, in conjunction with the equilibrium constants of reactions (1) and (2) obtained by spectrophotometry in this work, and the protonation constants and enthalpy of protonation of HEDTA from the literature, were fitted to calculate the enthalpies of complexation for NpO_2L^{2-} and NpO_2HL^-. As shown in Figure 2 (lower figure), excellent fit was obtained. The calculated enthalpies of complexation for NpO_2L^{2-} and NpO_2HL^- are listed in Table 1. In the pC_H range of the acid titrations, the ternary $(NpO_2)_2(OH)_2L_2^{6-}$ complex is negligible.

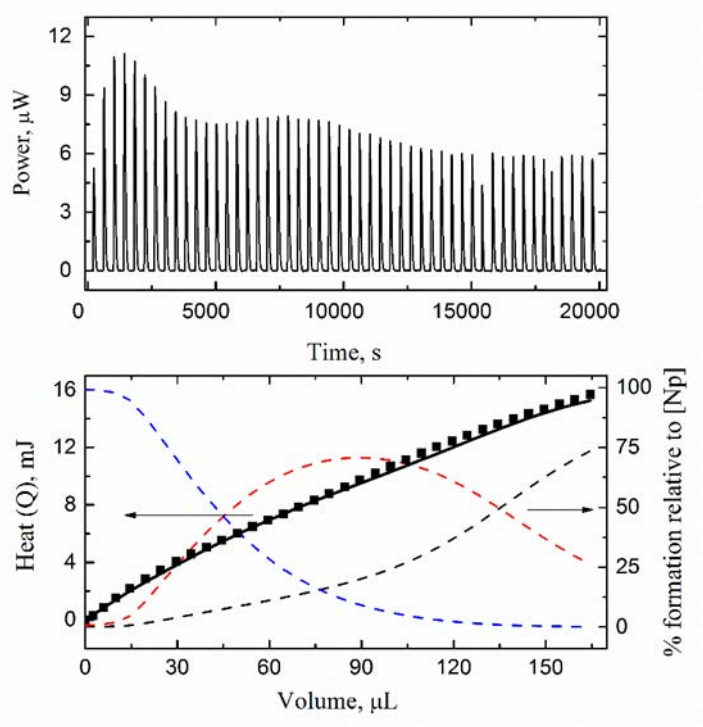

Figure 2. Calorimetric titration of NpO_2^+/HEDTA (t = 25 °C, I = 1.0 mol·L^{-1} $NaClO_4$). Upper figure: thermogram (dilution heat not corrected). Lower figure: observed (■) and calculated (-) total reaction heat (left y axis) and speciation of Np(V) (right y axis, dashed lines: NpO_2^+ (black), NpO_2L^{2-} (blue) and NpO_2HL^- (red)) as a function of titrant volume.

The data from the base titration that covered a wide pC_H range (up to 10.5) were fitted in two ways: a "global" fit for enthalpies of complexation for all three Np(V)/HEDTA complexes including the ternary $(NpO_2)_2(OH)_2L_2^{6-}$ complex, or a restricted fit by holding the enthalpies of complexation for NpO_2L^{2-} and NpO_2HL^- obtained from acid titrations as constants and fitting exclusively for $(NpO_2)_2(OH)_2L_2^{6-}$. None of the attempts were successful, this is most likely due to the combination of: (1) the titration cell of the calorimeter is in fact open to the atmospheric environment and the interference of carbon dioxide at high pC_H cannot be ignored; (2) the maximum percentage of $(NpO_2)_2(OH)_2L_2^{6-}$ in the titration was only ~ 10%, probably too little for accurate calculation. As a result, only the enthalpies of complexation for NpO_2L^{2-} and NpO_2HL^- are reported in Table 1. The corresponding entropies of complexation are also calculated

from the enthalpies and free energies. The values of enthalpy and entropy of complexation, the first such data determined for the Np(V)/HEDTA system, indicate that both enthalpy and entropy favor the complexation, but the entropy is the dominant driving force for the complexation due to the chelating effect of the aminopolycarboxylic acids.

2.1.3 Thermodynamic trends and possible coordination modes in Np(V) complexes with aminopolycarboxylic acids

As shown in Figure 3, excellent linear correlations are observed between the stability constants of ML and MHL complexes (where M stands for NpO_2^+) and the total basicity (i.e., ΣpK_a) of the related ligands, suggesting that the complexation of NpO_2^+ with the aminopolycarboxylic acids can be described by electrostatic interactions and the binding strength is directly related to the ligand basicity. In addition, the linearity of the correlation could imply that the coordination modes in the Np(V) complexes are probably similar for these ligands. However, as the following discussions suggest, while this could be true for the ML complexes of all aminopolycarboxylic acids, the coordination mode in the protonated complex (MHL) of the ligands with only one amino group (e.g., nitrilotriacetic acid (NTA) and IDA) could be different from that of the ligands with more than one amino group (e.g., HEDTA and EDTA). Possible coordination modes in ML and MHL complexes are discussed below.

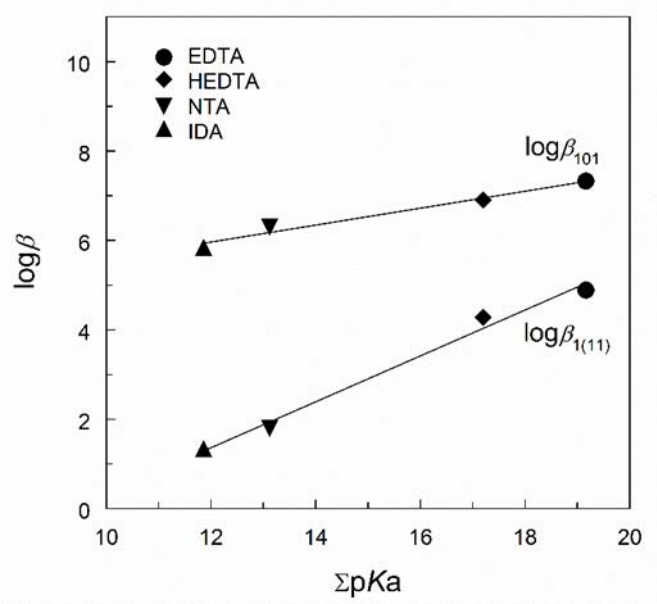

Figure 3. Stability constants vs. total ligand basicity (pK_a) at t = 25°C. logβ_{101} for NpO_2L^{2-} and log$\beta_{1(11)}$ for $NpO_2(HL)^-$; all values at I =1.0 mol·L^{-1} $NaClO_4$ except that of log$\beta_{1(11)}$ for Np(V)/IDA Np(V)/IDA at I = 0.1 mol·L^{-1} $NaClO_4$.

$NpO_2L^{(n-1)-}$. Due to the linear configuration of the NpO_2^+ ion, the ligands can only approach the center Np atom through the equatorial plane. A simpler trident ligand such as IDA could use all donor atoms, one N and two O atoms, to coordinate NpO_2^+, as shown in Figure 4(a). However, due to steric restrictions, ligands with higher denticity such as HEDTA and EDTA could only use some of the donor atoms, at most one N and two O atoms, to coordinate NpO_2^+ through the equatorial plane, as shown in Figure 4(b), leaving the other N atom and carboxylate groups not coordinated to the same Np center. Similar modes are suggested for the coordination of UO_2^{2+} with EDTA. This means that the local coordination environment of NpO_2^+ in the ML complexes with HEDTA, EDTA, NTA and IDA is similar as shown by Figure 4(a) and 4(b).

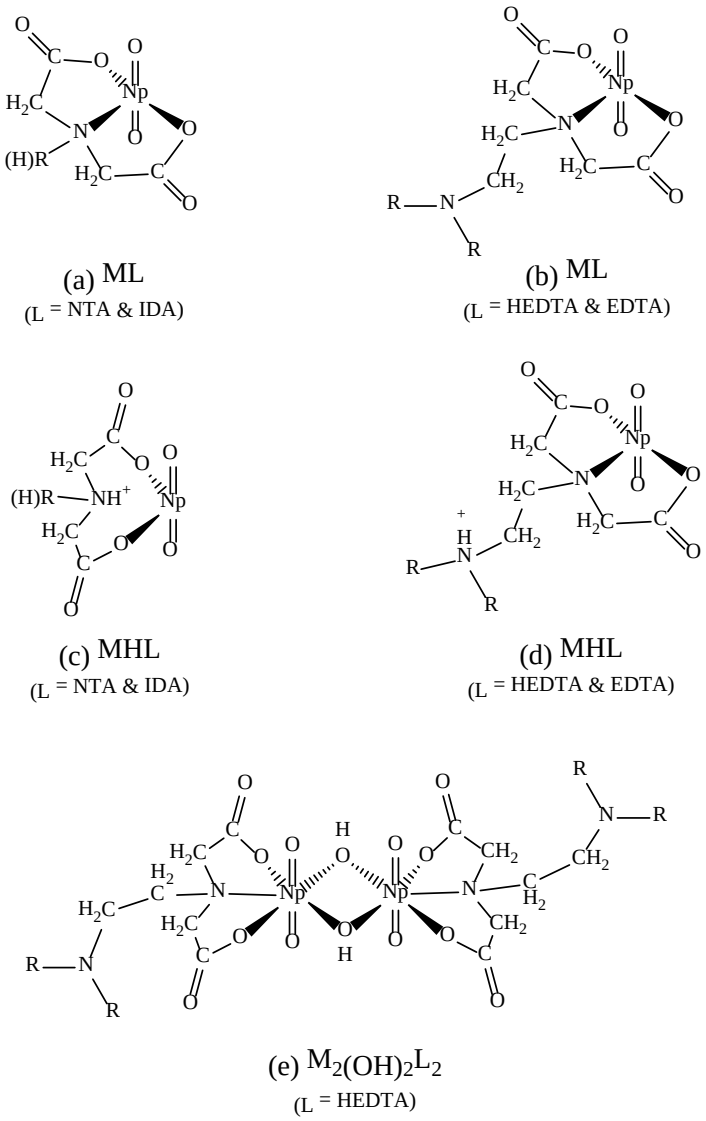

Figure 4. Possible coordination modes in the Np(V) complexes with aminopolycarboxylic acids. (a) ML complexes of NTA and IDA; (b) ML complexes of HEDTA and EDTA; (c) MHL complexes of NTA and IDA; (d) MHL complexes of HEDTA and EDTA; (e) $M_2(OH)_2L_2$ of HEDTA.

$NpO_2(HL)^{(n-2)-}$. To help discuss the possible coordination modes in the protonated complexes of Np(V) with aminopolycarboxylic acids, additional spectrophotometric titrations with Np(V) and NTA were performed at I = 1.0 mol·L^{-1} $NaClO_4$. The stability constants are listed in Table 1.

The formation of the protonated complex for HEDTA and NTA, $NpO_2(HL)^-$, is described by reaction (2). In general, the M(HL) complex is less stable than the ML complex for all aminopolycarboxylic acids shown in Table 1, which is understandable as the interactions are predominantly electrostatic in nature and ligand L^{n-} has a higher negative charge than ligand $HL^{(n-1)-}$. However, data in Table 1 indicate that the difference ($\log\beta_{101}$ - $\log\beta_{1(11)}$) for HEDTA and EDTA is much smaller than that for NTA and IDA: 2.4 – 2.6 for HEDTA and EDTA while 4.5 – 4.9 for NTA and IDA. Such contrast could probably help reveal

the coordination modes in the protonated MHL complexes of NpO_2^+ with the aminopolycarboxylic acids as discussed below.

NTA and IDA possess only one amino N atom but HEDTA and EDTA possess two N atoms. Therefore it is reasonable to envisage that the protonation of the ML complexes with NTA or IDA occurs on the amino N atom so that it becomes weakly bonded to Np or does not bind Np at all, as shown in Figure 4(c), which results in bidentate MHL complex (Figure 4(c)) is much weaker (more than 4 orders of magnitude in the stability constants) than the tridentate ML complex (Figure 4(a)). In contrast, the protonation of the ML complexes with HEDTA and EDTA could probably occur on the amino N atom that is not directly bonded with Np, as shown in Figure 4(d). In this case, the MHL complexes remain tridentate so that they are only slightly weaker (about 2 orders of magnitude in stability constants) than corresponding ML complexes with HEDTA and EDTA.

Comparison of the deconvoluted absorption spectra of the ML and MHL complexes for the Np(V)/HEDTA and Np(V)/NTA systems (Figure 5) provides further rationalization of the above discussion. Data in Figure 5 show that the positions of the absorption bands of the ML and MHL complexes are close for the Np(V)/HEDTA system (Figure 5(a)), but drastically different for the Np(V)/NTA system (Figure 5(b)). This observation is consistent with the above discussion that suggests the local coordination environment of Np in the MHL complex differs significantly from that in the ML complex for the NTA or IDA systems, but remains similar for the HEDTA or EDTA systems.

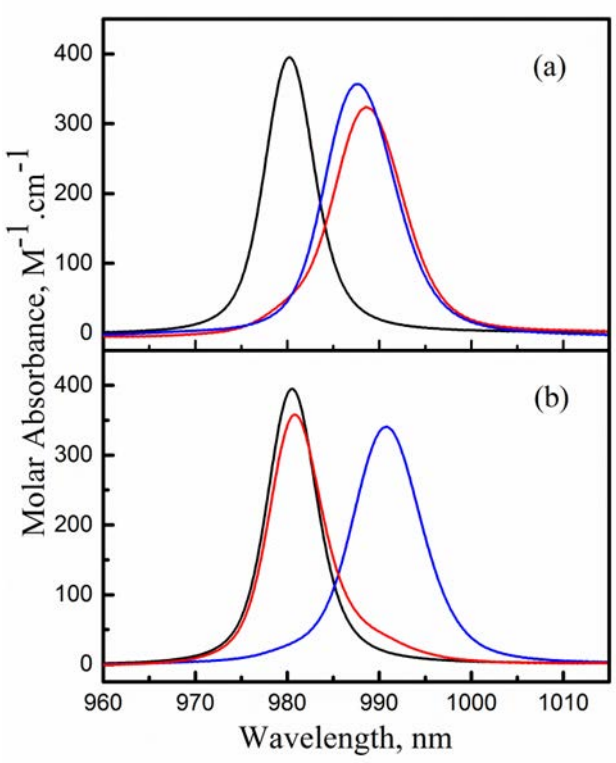

Figure 5. Resolved molar absorbance spectra of individual Np(V) species from the spectrophotometric titrations. (a) Np(V)/HEDTA, (b) Np(V)/NTA. NpO_2^+ (black), NpO_2L^{2-} (blue), NpO_2HL^- (red).

2.1.4 EXAFS results to coordination structures in Np(V)/HEDTA complexes

The k^3-weighted Np L_{III} EXAFS spectra and the? Fourier transform (FT) of three Np(V) solutions are presented in Figure 6. The fit lines are also depicted in the figure. Table 2 lists the structural fitting results as well as the Np(V) speciation of individual solutions. The FT represents a pseudo-radial distribution function, and the peaks are shifted to lower R values as a result of the phase-shifts associated with the absorber-scatter interactions (~0.2 - 0.5 Å). The speciation results indicate that the dominant Np(V) species are NpO_2^+ (100%), NpO_2L^{2-} (100%) and $(NpO_2)_2(OH)_2L_2^{6-}$ (87%) in solutions I, II and III, respectively, (L is denoted as fully deprotonated HEDTA). An excellent fit was achieved with the proposed coordination structures for those Np(V) species, the details of which are discussed below.

The EXAFS results of solution I well demonstrate that the dioxo Np(V) is surrounded by five oxygens (O_{eq}) in its equatorial plane with a distance of 2.51 Å ($R_{Np\text{-}Oeq}$). The distance of dioxo oxygen (O_{ax}) to Np(V) is 1.82 Å ($R_{Np\text{-}Oax}$). Those results are in excellent agreement with the early work on the structure of hydrated neptunyl in aqueous solution.

In the presence of HEDTA, the EXAFS features of Np(V) have varied. The variation provide information on the coordination structures of the Np(V)/HEDTA complexes. For solutions II, the peak at 2.0 Å in its FT graph, which is supposed to form from the scattering of equatorial coordination atoms, was largely broadened. Also, a new peak appeared at 2.5 Å. The fitting indicates that this new peak is attributed to the single scattering of Np to one nitrogen atom (N_{eq}) in its equatorial coordination plane. And the broadened peak at 2.0 Å corresponds to the single scattering of Np to four O_{eq}s but with a large Debye-Waller factor (σ^2 = 0.0114, Table 2). The unusually large Debye-Waller factor may suggest that this scattering shell is composed of two coordination shells, which could not be resolved due to the limited *k* range available in the data. The resultant $R_{Np\text{-}Oeq}$ values of solutions I and II also support the above argument. As indicated in Table 2, the $R_{Np\text{-}Oeq}$ of solution II is 2.41 Å, and much shorter than that of solution I. The smaller $R_{Np\text{-}Oeq}$ with the large Debye-Waller factor implies that this scattering shell may be composed of some oxygens from the hydrated water molecules and the others from the coordinated HEDTA. The oxygens from the HEDTA could bind to Np(V) more closely to those from the water, thereby forming two coordination shells. Taking into consideration the fact that one nitrogen participates in the coordination, it is most likely that in the Np(V)/HEDTA complex (NpO_2L^{2-}), the HEDTA tridentately coordinates to Np(V) through two oxygens from two carboxylates and one nitrogen from the amine group. This is in excellent agreement with the coordination mode yielded from the thermodynamic trends of Np(V) complexation with aminopolycarboxylic acids.

The EXAFS of solution III presents interesting features, evidently confirming the proposed complexation model and coordination mode in the Np(V)/HEDTA complex ($(NpO_2)_2(OH)_2L_2^{6-}$) formed at high pH. The features include: (1) A new peak occurred at 3.5 Å; (2) the peak at 2.0 Å became much sharper, compared to that of solution II (c.f. Figure 6). Those features are well fitted with the following scattering shells: Np-O_{eq} (coordination number: 3.7), Np-N_{eq} (1.0) and Np-Np (1.0). The presence of the Np-Np shell strongly demonstrates a formation of the dimeric Np(V) species, which has been proposed from our spectrophotometry work. The sharpness of the Np-O_{eq} peak suggests that this dimeric species is likely to form through double-OH bridging as described in Figure 4(e). Unlike a water molecule, hydroxide is a strong complexing agent so that the bond length of metal to oxygen of hydroxide is shorter than that of metal to oxygen of water. Also, the early work has confirmed that the hydrolysis of metal cations could weaken the binding strength between metals and organic ligands, thereby increasing the metal-ligand bond length. Those two factors together may generate the scenario that for each Np(V) center in this dimeric complex, two oxygens from HEDTA (tridentate coordination mode) and two oxygens from hydroxides (double-OH bridging) coordinate to Np(V) with the same or similar bond length, resulting in a simple single scattering shell. Therefore, we came to the conclusion that this ternary Np(V)-OH-HEDTA complex is a dimeric Np(V) species through double-OH bridging, and in the complex, each HEDTA maintains a tridentate coordination mode (Figure 4(e)).

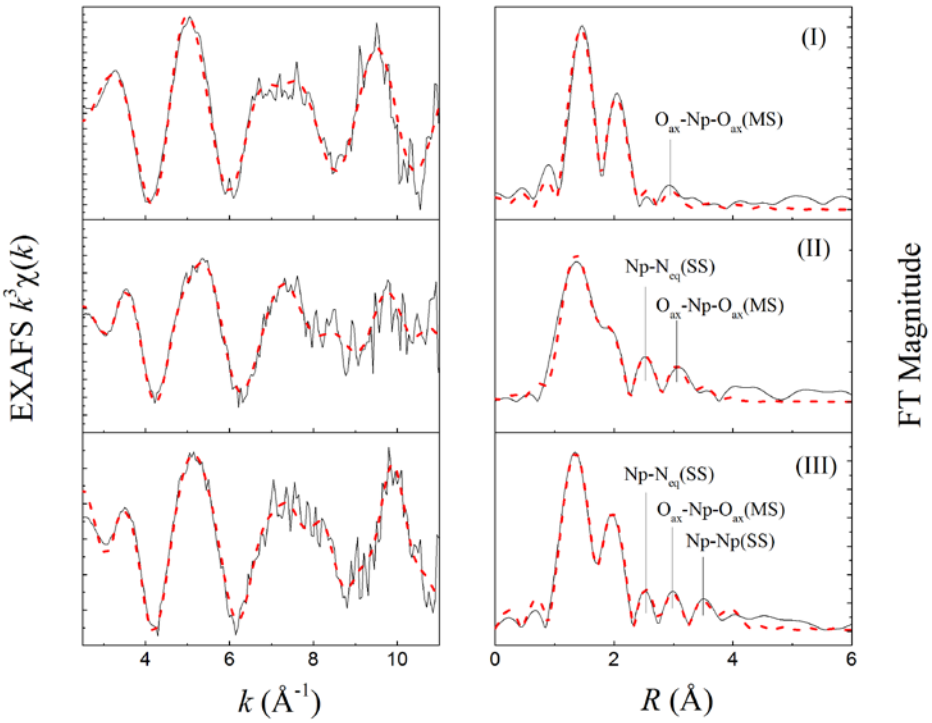

Figure 6. Np L_{III} EXAFS of three Np(V) solutions. (I) [Np] = 3.0 mmol·L^{-1}, pC_H = 2.5; (II) [Np] = 1.0 mmol·L^{-1}, [HEDTA] = 2.3 mmol·L^{-1}, pC_H = 9.4; (III) 2.0 mL, [Np] = 1.0 mmol·L^{-1}, [HEDTA] = 23 mmol·L^{-1}, pC_H = 12. Black solid line – experimental, red dash line – fit.

Table 2 EXAFS fitting results of Np(V) species in solutions from this work

Solution[a]	Shell	N	R (Å)	σ^2	Notice
I	Np-O_{ax}	2.0	1.82	0.0025	S_0^2 = 0.85, ΔE^0 = 5.56 eV
Speciation: 100% NpO_2^+	Np-O_{eq}	4.6	2.51	0.0096	r = 0.005, χ^2_{red} = 13.0
II	Np-O_{ax}	2.0	1.82	0.0046	
Speciation: 100 % NpO_2L^{2-} (L = HEDTA)	Np-O_{eq}	3.8	2.41	0.0114	S_0^2 = 075, ΔE^0 = 8.05 eV r = 0.004, χ^2_{red} = 14.5
	Np-N_{eq}	1.0	3.95	0.0047	
III	Np-O_{ax}	2.0	1.82	0.0038	
	Np-O_{eq}	3.7	2.40	0.0089	
Speciation: 11% NpO_2L^{2-} 87 % $(NpO_2)_2(OH)_2L_2^{6-}$	Np-N_{eq}	1.0	2.93	0.0039	S_0^2 = 0.77, ΔE^0 = 9.01 eV r = 0.005, χ^2_{red} = 15.1
	Np-Np	1.0	3.95	0.0046	

[a] The Np(V) speciation (relevant to total [Np]) was calculated with the simulation program HySS2009 using the complexation constants determined in this work.

3. CONCLUSION

Three Np(V) complexes with HEDTA, NpO_2L^{2-}, NpO_2HL^{-}, and $(NpO_2)_2(OH)_2L_2^{6-}$, were included in the modelling of spectrophotometric titration data. The hydrolyzed dimeric species, $(NpO_2)_2(OH)_2L_2^{6-}$, becomes significant in the high pH region. Data by EXAFS provide support for the presence of this species in aqueous solutions of high pH.

4. PUBLICATIONS

Xingliang Li, Zhicheng Zhang, Leigh R. Martin, Shunzhong Luo, Linfeng Rao, Complexation of NpO_2^{+} with (2-Hydroxyethyl) ethylenediaminetriacetic Acid (HEDTA) in Aqueous Solutions: Thermodynamic Studies and Structural Analysis, *RSC Advances*, in review.

5. ACKNOWLEDGMENTS

Funding for this work was provided by the Fuel Cycle Research and Development Program, Materials Recovery and Waste Form Development Campaign, Office of Nuclear Energy, of the U.S. Department of Energy under Contract Number DE-AC02-05CH11231 with Lawrence Berkeley National Laboratory.